Lane-based Estimation of Travel Time Distributions by Vehicle Type via Vehicle Re-identification Using Low-resolution Video Images

Cheng Zhang[a], H. W. Ho[b], William H. K. Lam[b]*, Wei Ma[b], S. C. Wong[c] and Andy H. F. Chow[d]

[a] *Department of Traffic Engineering, University of Shanghai for Science and Technology, Shanghai, China;*

[b] *Department of Civil and Environmental Engineering, The Hong Kong Polytechnic University, Kowloon, Hong Kong, China;*

[c] *Department of Civil Engineering, The University of Hong Kong, Hong Kong, China;*

[d] *Department of Advanced Design and Systems Engineering, City University of Hong Kong, Kowloon, Hong Kong, China;*

The ORCIDs of authors

Cheng Zhang:	0000-0002-6529-2468
H. W. Ho:	0000-0002-9072-9959
William H. K. Lam:	0000-0002-7625-3712
Wei Ma:	0000-0001-8945-5877
S. C. Wong:	0000-0003-1169-7045
Andy H. F. Chow:	0000-0002-2877-357X

* Corresponding author. E-mail: william.lam@polyu.edu.hk

(Word count 11,271)

Lane-based estimation of travel time distributions by vehicle type via vehicle re-identification using low-resolution video images

Travel time estimation plays an essential role in the high-granular traffic control and management of urban roads with distinct lane-changing conditions among lanes. However, little attention has been given to the estimation of distributions of travel times among different lanes and different vehicle types in addition to their expected values. This paper proposes a new method for estimating lane-based travel time distributions with consideration of different vehicle types through matching low-resolution vehicle video images taken by conventional traffic surveillance cameras. The vehicle type classification is based on vehicle sizes and deep learning features extracted by densely connected convolutional neural networks, and the vehicle re-identification is conducted through a lane-based bipartite graph matching technique. A case study is carried out on a congested urban road in Hong Kong. Results show that the proposed method performs well in estimating the lane-level travel time distributions by vehicle type which can be very helpful for various lane-based and vehicle type-specific traffic management schemes.

Keywords: lane-based travel time distribution, vehicle type, vehicle re-identification, lane changing behaviors, video images

1. Introduction

Travel time information is a crucial requirement for many Intelligent Transportation Systems (ITS) applications, such as traffic monitoring, traffic management and path navigation. However, in real world, comprehensive and extensive travel time information on urban roads may not be available due to the limitation of existing traffic detectors/video cameras installed in urban road networks (Chen et al., 2016; Tam & Lam, 2011). Due to site constraints especially in densely developed urban areas in Hong Kong, it is difficult to set up video cameras at upstream and downstream locations with the same/similar angles of view, as illustrated in Figure 1. Also, license plate numbers of vehicles cannot be identified from the low-resolution video images.

{Insert Figure 1 here}

The provision of lane-based travel time information is important for urban roads, because different lanes of the same road segment may have distinctive traffic conditions. As illustrated in Figure 1, there was a long queue in Lane 4 (the far-side lane) while other lanes were less congested. A lane-based travel time estimation can clearly distinguish such differences, so that path navigation can provide more accurate travel time information for vehicles in different lanes. Additionally, urban roads have more frequent lane changes and various vehicle types. An accurate estimation of the lane-based travel time by vehicle type can help to better understand the lane-changing effects by vehicle type, which provides support for traffic management of lane-changing behaviors (e.g. using lane markings). Therefore, it is necessary to estimate the lane-based travel times by vehicle type with use of the low-resolution video images from different angles of view.

Various methods of travel time estimation have been developed for different data sources (Mori et al., 2015). Owing to the wide deployment of point detectors, typically loop detectors, a variety of methodologies were based on speed, flow and occupancy data collected at fixed points (Celikoglu, 2013; Li et al., 2006). However, traffic states vary significantly at different locations along a congested urban road. Point detector data cannot represent the whole road section (Soriguera & Robusté, 2011). Therefore, travel time estimations based on point detector data do not perform well under congestion (Jiang et al., 2017).

Probe vehicles with Global Positioning Systems (GPS) or cell phones can collect position and speed data at a regular time interval (e.g., 30 seconds). Using GPS data, vehicles can be tracked and travel time data of vehicle samples between two positions can be obtained. This brings more information for travel time estimation. Nevertheless, sparse GPS data are common in real world (Prokhorchuk et al., 2020; Sanaullah et al.,

2016). Besides the low sampling frequency, it is usual that GPS data are only available from specific vehicle types such as taxis (Jenelius & Koutsopoulos, 2013) and buses (Uno et al., 2009). Moreover, GPS positional accuracy usually cannot reach the lane level. With the advancement of sensing and communication technologies, the collection of lane-level vehicle trajectories will become possible under connected vehicle environments. However, such data are not yet available on most urban roads (Lu et al., 2021).

Interval detectors are composed of a pair of detectors deployed at two fixed locations. They are capable to match the same vehicle at different locations, which enables direct collection of travel time data between two locations. Using automatic vehicle identification (AVI) techniques (Tam & Lam, 2011) or Bluetooth technologies (Araghi et al., 2016), vehicle matching can be easy as each vehicle has a unique identifier (e.g., a Media Access Control address in the case of Bluetooth). However, the low penetration rate and limited number of fixed detectors limit the number of valid matching data for travel time estimation in practice.

Vehicle re-identification (V-ReID) is another important technique of interval detectors to obtain travel time data (Yu et al., 2015). It is to match the same vehicle at different locations by vehicle features (e.g. length and type) rather than unique identifiers. As anonymous approaches, V-ReID techniques have been developed for various detectors/sensors, including loop detectors (Coifman & Cassidy, 2002), video cameras (Sun et al., 2004), wireless magnetic sensors (Kwong et al., 2009) and weigh-in-motion sensors (Basar et al., 2018). Owing to the wide deployment of video cameras in many cities around the world, video-based V-ReID has received much attention recently for real-time traffic data collection (Khan & Ullah, 2019). Visual features such as color, length, and type of the recorded vehicles can be captured by most video cameras (Sumalee et al., 2012). With a high-resolution camera and carefully set-up camera views, license

plate numbers (Oliveira-Neto et al., 2012) and other specific features such as annual inspection labels, tissue boxes, and ornaments (Bai et al., 2018) can be captured for V-ReID. However, the use of these features in V-ReID may not be practical owing to privacy issues and the limited availability of high-resolution video images in reality. Besides travel time data collected through V-ReID, heterogeneous data fusion has also received attention for more accurate travel time estimation (Fu et al., 2019; Guo & Yang, 2020; Li et al., 2016; Shi et al., 2017).

Recently, there has been increasing interests in not only mean travel time estimation but also the estimation of standard deviation and travel time distributions, especially for urban road networks (Lu et al., 2021; Prokhorchuk et al., 2020; Shi et al., 2017; Zheng & Van Zuylen, 2014). Parametric models, e.g. Gaussian mixture models (Tang et al., 2020; Yang et al., 2017), and non-parametric models, e.g. kernel density estimation (Chiou et al., 2021; Duan et al., 2020), have been employed to estimate travel time distributions. Spatial-temporal correlations between road links have been taken into consideration using Markov chains (Ma et al., 2017; Tang et al., 2020) and copula models (Chen et al., 2018; Samara et al., 2021; Yun et al., 2019). Other advanced models, such as Bayesian probabilistic model (Tang et al., 2018), Generative Adversarial Network (Zhang et al., 2019) and Monte Carlo Simulation (Filipovska et al., 2021), have also been applied to the estimation of travel time distributions.

Nevertheless, little attention has been given to estimate travel time distributions for different types of vehicles traveling in different lanes particularly on urban roads with various lane-changing maneuvers. However, it is important to distinguish travel time distribution by traffic lane and vehicle type for different traffic management purposes in practice. For example, these information can be very helpful to determine the entry and exit locations of bus-only lane; to change lane markings for controlling the

merging/diverging of different vehicles; and to estimate the traffic emission/fuel consumption by vehicle types etc.

As summarized in Table 1, most of the existing methods failed to distinguish the differences of travel times by traffic lane on road segments. Lu et al. (2021) estimated lane-level travel time distributions using connected vehicles data in a simulation testbed, but the unavailability of real-world data limits their application. Zhang et al. (2021) utilized real video images to estimate lane-level travel time distributions but they did not distinguish their results by vehicle types.

{Insert Table 1 here}

To fill the aforementioned gaps, this study extends Zhang et al. (2021)'s work to estimate lane-level travel time distributions by vehicle type using widespread low-resolution video images on urban roads but from different angles of view. As illustrated in Figure 2, the travel time is estimated via vehicle re-identification (V-ReID) using video images collected at selected upstream and downstream locations. The lane locations of vehicles are identified and vehicle types are classified based on vehicle images to enable travel time estimation in a more detailed and fine-grained manner. In contrast to the existing literature, the method of estimating travel times proposed in this study aims to find the actual travel times instead of the instantaneous travel times of vehicles passing through an urban road network.

{Insert Figure 2 here}

The rest of this paper is organized as follows. Section 2 briefly describes related work on vehicle re-identification using low-resolution video images from different angles of view, Section 3 introduces the proposed lane-based travel time estimation by vehicle type, Section 4 presents experiments for the analysis of the performance of the proposed

method, and Section 5 summarizes the main findings of the study and provides recommendations for further research.

2. Related work

Due to the wide deployment of video surveillance cameras in many cities, a lot of video-based V-ReID methods have been proposed. The V-ReID is to identify each vehicle in upstream video images and to re-identify the same vehicle in downstream video images, as illustrated in Figure 2. Based on the V-ReID results, the actual travel times of all re-identified vehicles are collected for travel time estimation. The framework of travel time estimation via V-ReID includes four major steps as follows.

2.1 Step 1: Vehicle feature extraction

For all vehicles passing through the upstream section (U) and downstream section (D), their vehicle features including vehicle color (C), vehicle type (T), vehicle length (L), arrival time (τ) and spot speed (v) are extracted using video image processing techniques (Sun et al., 2004; Wang et al., 2014). Each upstream vehicle $i \in U$ is then represented by $(C_i^U, T_i^U, L_i^U, \tau_i^U, v_i^U)$ and each downstream vehicle $j \in D$ is represented by $(C_j^D, T_j^D, L_j^D, \tau_j^D, v_j^D)$.

2.2 Step 2: Construction of travel time window

A travel time window refers to the lower bound (Lb) and upper bound (Ub) of expected travel times. In most V-ReID studies, the travel time window $[Lb, Ub]$ has been adopted to determine the search space of candidate vehicle matches. The time difference between feasible vehicle matches (i, j) should satisfy the constraint of travel time window, i.e. $\tau_j^D - \tau_i^U \in [Lb, Ub]$, where τ_i^U is the arrival time of vehicle i at the upstream section and τ_j^D is the arrival time of vehicle j at the downstream section.

The construction of travel time window is important because it affects the number of vehicles within the search space. If the range of travel time window is too large, too many candidates will reduce the possibility of finding the correct match. On the contrary, if the range of travel time window is too small, the correct match may be filtered out from the search space. Thus, appropriate travel time windows should be constructed for V-ReID. Fixed travel time windows have been determined according to historical travel time distribution of study sites (Basar et al., 2018; Sumalee et al., 2012). An adaptive strategy was further introduced to adjust travel time windows depending on real-time traffic conditions (Wang et al., 2014).

2.3 Step 3: Vehicle matching

Within the search space, vehicle matching is to determine optimal matches between upstream and downstream vehicles based on their vehicle similarities. In general, the calculation of similarity between an upstream vehicle and a downstream vehicle can be classified into two categories: distance-based methods and probabilistic methods. Distance-based methods describe the similarities of candidate vehicle pairs for re-identification through various distance measures of vehicle features, such as color features, type features, length features and deep learning features (Sun et al., 2004; Tang et al., 2018).

Probabilistic methods have been proposed to address the issue of measurement noise of vehicle features (Kwong et al., 2009). Rather than a deterministic distance measure, a matching probability is calculated for two vehicles using a Bayesian model. In addition to the matching probability determined by distance measures from vehicle features, the historical or real-time estimated travel time distribution was regarded as a prior matching probability in determining the posterior probability to be used for V-ReID (Sumalee et al., 2012; Wang et al., 2014). The lane changing probability of vehicles

between upstream and downstream locations was also incorporated for V-ReID (Zhang et al., 2021).

This vehicle matching problem is then formulated as a bipartite graph matching problem (Sumalee et al., 2012; Wang et al., 2014; Zhang et al., 2021). In this bipartite graph, the upstream and downstream vehicle sets are represented by two parts of vertices. The edges between two vertices refer to the similarity between two vehicles. The optimal matching aims to maximize overall similarities of the bipartite graph. To improve the accuracy of vehicle matching, vehicle platoons are re-identified for each lane under the assumption that vehicles seldom change lanes between upstream and downstream locations (Coifman & Cassidy, 2002; Sun et al., 2004).

2.4 Step 4: Travel time estimation

Based on the vehicle matching results, the travel time is determined by the time difference of matched, or re-identified, vehicles detected at selected upstream and downstream locations. These travel time samples are utilized for travel time estimation.

2.5 Discussion on existing methods

The existing methods can provide reasonable estimations of mean travel times on freeways. Under the assumption that vehicles seldomly change lanes in a freeway section, vehicle can be re-identified for each lane and thus candidate vehicle matches are substantially reduced. However, this assumption may not be valid for urban roads with frequent lane changing movements. Moreover, for urban roads, frequent lane changes and the mix of different vehicle types are common. As such, travel time variations are larger by lane and vehicle type. Thus, following the existing methods, the range of the travel time window for re-identification may be large, which poses challenges in V-ReID for travel time estimation as they increase the likeliness of incorrect matching. The high

similarity of different vehicles (e.g., sedans produced by the same manufacturer and taxis) and the difference in appearance of the same vehicle as viewed by the upstream and downstream cameras (with the upstream camera capturing the front of the vehicle and the downstream camera capturing the back) also brings challenges. Consequently, travel time samples resulted from the existing methods are not sufficient for lane-based estimation of travel time distributions by vehicle type.

This study aims to estimate lane-level travel time distributions by vehicle type using widespread low-resolution video images on urban roads with different angles of view at the upstream and downstream locations. The key contributions of this study are summarized as follows. A lane-based travel time estimation framework is proposed for different vehicle types, which considers lane changing behaviors, to model the travel time distributions in different lanes for different types of vehicles. The proposed method re-identifies vehicles more accurately by adopting a lane-based time window approach. The use of the lane-based time window screens out invalid vehicles more efficiently and thus improves the accuracy of the travel time estimation with consideration of the spatial-temporal information of upstream and downstream locations. Travel time distributions and the probability of the downstream lane used by a vehicle, which are estimated from the vehicles' lane changing behaviors upstream, are considered as the prior knowledge together with visual features (e.g., the vehicle color, length, and type) extracted from video images with different angles of view for calculating the matching probability. An optimal matching problem, which maximizes the matching probabilities, is formulated and solved to re-identify the vehicles. In addition, vehicle type classification is proposed based on vehicle sizes and deep learning features of vehicle images.

3. Methodology

The proposed method simultaneously classifies vehicles into different vehicle types and re-identifies them by matching low-resolution video images taken at selected upstream and downstream locations. The proposed method for vehicle classification and re-identification comprises five major steps; a flowchart of the proposed framework is shown in Figure 3. Step 1 extracts the vehicle features and information to be used in the classification and re-identification in the later steps. With the extracted vehicle features, Step 2 classifies the vehicles identified in Step 1 into different vehicle types. Step 3 determines the lane-based travel time windows at the downstream location to serve as the search space for the efficient V-ReID to be carried out in Step 4. With the re-identification results from Step 4, the lane-based travel time distributions of different types of vehicles are estimated in Step 5. Details of the five steps are described in the following sub-sections.

{Insert Figure 3 here}

3.1 Step 1: Vehicle feature extraction

With the use of video image processing techniques, all of the vehicles passing through the upstream and downstream sections are identified (see Figure 2) and their vehicle visual features and mobility statuses are extracted. The extracted visual features of the vehicles are the vehicle color (C), vehicle type (T), and vehicle length (L) and the extracted mobility statuses of the vehicles are the arrival time (τ), lane location (l), spot speed (v), and lane changing pattern (LC). Compared to the existing methods, lane location (l) and lane changing pattern (LC) are also extracted for the proposed lane-based framework.

The proposed methodology integrates the You Only Look Once (YOLOv3) algorithm for vehicle detection (Redmon & Farhadi, 2018) and the Deep Simple Online

and Realtime Tracking (Deep SORT) algorithm for multiple-vehicle tracking using the same camera view (Wojke et al., 2017). Images of the detected vehicles are extracted from the video and analyzed for the extraction of the visual features (Wang et al., 2014). The mobility statuses of each vehicle in the upstream and downstream locations are extracted by tracking the vehicle's trajectory in the corresponding video using Deep SORT. On the basis of the above analysis carried out through image processing, a set of vehicles in the upstream section (U) is identified, and each upstream vehicle i (i.e., $i \in U$) is then represented by $(C_i^U, T_i^U, L_i^U, \tau_i^U, l_i^U, v_i^U, LC_i^U)$. Similarly, a set of vehicles in the downstream section (D) is identified, and each downstream vehicle j (i.e., $j \in D$) is represented by $(C_j^D, T_j^D, L_j^D, \tau_j^D, l_j^D, v_j^D)$.

3.2 Step 2: Vehicle type classification

In this step, template matching, which is based on the distance measures—or similarity—of the given vehicle image and the template images of different vehicle types, is adopted for vehicle type classification. In this study, features extracted/learned from the vehicle images and vehicle length are simultaneously considered in the template matching. Densely Connected Convolutional Networks (DenseNet), which has shown good performance in computer vision (Huang et al., 2017), is adopted to extract deep learning features (denoted by $\mathcal{F}$) from the image of a detected vehicle and to compare those features with features extracted from the template images. The vehicle length (L) is represented by the image height of the captured vehicle, which is normalized for different viewing angles of the upstream and downstream cameras (Zhang et al., 2021).

For each vehicle type (e.g., sedans, minibuses, or trucks), multiple template images are included to ensure a wide variety of vehicle features (e.g., color and shape). This is considered to enhance the classification accuracy. Suppose that $Tem_{\kappa,x}$ is a template

image for vehicle type κ and image index x. Then, given a vehicle image I, the distance measures of this image (I) and template x of vehicle type κ ($Tem_{\kappa,x}$) can be calculated. For each vehicle type κ ($x = 1, \ldots N_{tem}$), the distance measure of vehicle image I relative to vehicle type κ is taken as an average of these N_{tem} template images. The distance measure for a deep learning feature, $D_{\mathcal{F}}(\kappa)$, is thus defined as

$$D_{\mathcal{F}}(\kappa) = \underset{x=1,\ldots N_{tem}}{\text{avg}} \left(\left\| \mathcal{F}(I) - \mathcal{F}\left(Tem_{\kappa,x}\right) \right\|^2 \right) \quad (1)$$

where $\mathcal{F}(I)$ and $\mathcal{F}\left(Tem_{\kappa,x}\right)$ are respectively the deep learning features for vehicle image I and template image $Tem_{\kappa,x}$. The distance measure of vehicle length, $D_L(\kappa)$, is defined as

$$D_L(\kappa) = \underset{x=1,\ldots N_{tem}}{\text{avg}} \left(\left\| \frac{L(I) - L\left(Tem_{\kappa,x}\right)}{L\left(Tem_{\kappa,x}\right)} \right\|^2 \right) \quad (2)$$

where $L(I)$ and $L\left(Tem_{\kappa,x}\right)$ are respectively the vehicle lengths for vehicle image I and template image $Tem_{\kappa,x}$. The overall distance measure, $D(\kappa)$, is defined as the weighted sum of the above two distance measures $D_{\mathcal{F}}(\kappa)$ and $D_L(\kappa)$:

$$D(\kappa) = D_{\mathcal{F}}(\kappa) \cdot (1 - w) + D_L(\kappa) \cdot w \quad (3)$$

where w is the fusion weight of the vehicle length. The number of template images (N_{tem}) and the fusion weight (w) are then calibrated using the training dataset. The objective is to find the optimal values of N_{tem} and w such that the classification accuracy, Acc_t, is maximized.

Using the calibrated parameters (N_{tem} and w) and extracted features ($\mathcal{F}$ and L), a distance measure $D(\kappa)$ can be calculated for a given vehicle image (I) relative to each

vehicle type κ. A vehicle, which gives the vehicle image (I), is then assigned to the vehicle type with the minimum distance measure (or maximum similarity):

$$Type(I) = \underset{\kappa}{\operatorname{argmin}}\, D(\kappa) \tag{4}$$

We categorize the vehicles into six types, namely sedans, taxis, vans, minibuses, trucks, and buses. Thus, for each vehicle image, six distance measures (i.e., $D(\kappa),\ \forall \kappa \in [1,6]$) are calculated. The distance measures relative to all six vehicle types of the vehicle image in Table 2 are calculated using Equation (1) – (3) and given in the same table. This vehicle is classified as a truck as it has the minimum distance measure (0.9241) relative to truck templates.

{Insert Table 2 here}

3.3 Step 3: Construction of lane-based travel time windows

This step constructs lane-based travel time windows, or ranges of travel time between the upstream and downstream sections. The constructed travel time windows help to delimit feasible matches between upstream and downstream vehicles. This extends the previous link-based travel time window construction step (Wang et al., 2014) by explicitly considering distinct traffic conditions in different lanes.

For each lane l and each time period t, a travel time window $\left[\widetilde{Lb}_{l,t}, \widetilde{Ub}_{l,t}\right]$, where $\widetilde{Lb}_{l,t}$ and $\widetilde{Ub}_{l,t}$ are respectively the lower and upper bounds of the travel time window, is derived from the predicted travel time distribution $\tilde{T}_{l,t}(\tilde{\mu}_{l,t}, \tilde{\sigma}_{l,t}, \tilde{\pi}_{l,t})$, with $\tilde{\mu}_{l,t}$, $\tilde{\sigma}_{l,t}$, and $\tilde{\pi}_{l,t}$ respectively being the mean, standard deviation, and type (e.g., normal or lognormal) of the predicted travel time for lane l and each time period t. With the predicted travel time distribution ($\tilde{T}_{l,t}$) for lane l and period t and the required confidence interval (α), the corresponding travel time window $\left[\widetilde{Lb}_{l,t}, \widetilde{Ub}_{l,t}\right]$ is defined

as $\left[\Phi^{-1}_{\tilde{T}_{l,t}}(\frac{1-\alpha}{2}), \Phi^{-1}_{\tilde{T}_{l,t}}(\frac{1+\alpha}{2})\right]$, with $\Phi^{-1}_{\tilde{T}_{l,t}}(\cdot)$ being the inverse of the cumulative distribution function of $\tilde{T}_{l,t}$.

For the predicted travel time ($\tilde{T}_{l,t}$) following a normal distribution, the travel time window, $\left[\widetilde{Lb}_{l,t}, \widetilde{Ub}_{l,t}\right]$, is defined as

$$\left[\widetilde{Lb}_{l,t}, \widetilde{Ub}_{l,t}\right] = \left[\tilde{\mu}_{l,t} + \mathrm{z}(\frac{1-\alpha}{2})\tilde{\sigma}_{l,t}, \tilde{\mu}_{l,t} + \mathrm{z}(\frac{1+\alpha}{2})\tilde{\sigma}_{l,t}\right] \quad (5)$$

where $\mathrm{z}(\cdot)$ is the z-score at a given confidence level which can be obtained from the standard normal distribution table.

Otherwise, if $\tilde{T}_{l,t}$ follows a lognormal distribution, the travel time window, $\left[\widetilde{Lb}_{l,t}, \widetilde{Ub}_{l,t}\right]$, is defined as

$$\left[\widetilde{Lb}_{l,t}, \widetilde{Ub}_{l,t}\right] = \left[e^{\tilde{\mu}^{\log}_{l,t} + \mathrm{z}(\frac{1-\alpha}{2})\tilde{\sigma}^{\log}_{l,t}}, e^{\tilde{\mu}^{\log}_{l,t} + \mathrm{z}(\frac{1+\alpha}{2})\tilde{\sigma}^{\log}_{l,t}}\right] \quad (6)$$

where $\tilde{\mu}^{\log}_{l,t}$ and $\tilde{\sigma}^{\log}_{l,t}$ are respectively the mean and standard deviation of the logarithm of $\tilde{T}_{l,t}$.

Given the arrival time of vehicle i in the upstream section (τ^U_i), the feasible arrival time window for the downstream lane l is determined as $\left[\tau^U_i + \widetilde{Lb}_{l,t}, \tau^U_i + \widetilde{Ub}_{l,t}\right]$. Accordingly, the set of feasible matches in downstream lane l of upstream vehicle i is denoted by $S_l(i)$ and expressed as

$$S_l(i) = \left\{j \middle| \tau^D_j \in [\tau^U_i + \widetilde{Lb}_{l,t}, \tau^U_i + \widetilde{Ub}_{l,t}]\right\} \quad (7)$$

where τ^D_j is the arrival time of vehicle j in the downstream section. The whole set of feasible matches in the downstream section, $S(i)$, is obtained as the union of $S_l(i)$ for all of the lanes.

3.4 Step 4: Lane-based bipartite graph matching

This step determines optimal matches between upstream and downstream vehicles using a lane-based bipartite graph matching technique. First, a matching probability P_{ij} is calculated for each feasible vehicle match (i, j) within the search space $S(i)$ as defined by Equation (7). Adopting the Bayesian approach, the matching probability P_{ij} is formulated as

$$P_{ij} = P\left(\delta_{ij} = 1 \middle| d_{ij}\right) = \frac{P\left(d_{ij}|\delta_{ij}=1\right)P\left(\delta_{ij}=1\right)}{P(d_{ij})} \quad (8)$$

where δ_{ij} denotes whether vehicles i and j match; i.e., $\delta_{ij} = 1$ indicates that vehicle i in the upstream section matches vehicle j in the downstream section and $\delta_{ij} = 0$ indicates that the vehicles *i* and *j* do not match. d_{ij} is the dis-similarity measures of these two vehicles based on their visual features of color (C), type (T), and length (L) (Wang et al., 2014). The calculation of P_{ij} depends on likelihood functions $P\left(d_{ij}\middle|\delta_{ij} = 1\right)$ and $P\left(d_{ij}\middle|\delta_{ij} = 0\right)$ and the prior probability function $P\left(\delta_{ij} = 1\right)$. The likelihood functions, $P\left(d_{ij}\middle|\delta_{ij} = 1\right)$ and $P\left(d_{ij}\middle|\delta_{ij} = 0\right)$, can be calibrated using the visual features, i.e. the color (C), type (T) and length (L), of the matched vehicle pairs from the training dataset. Apart from the probability defined by vehicle features ($P\left(d_{ij}\middle|\delta_{ij} = 1\right)$ and $P\left(d_{ij}\middle|\delta_{ij} = 0\right)$), this study also considers the probability of the two vehicles (i.e., vehicle i upstream and vehicle j downstream) being the same vehicle in a spatial and temporal manner. The prior probability $P(\delta_{ij} = 1)$ is the probability that the detected vehicles i and j are the same vehicle given their lane locations and arrival time at the upstream (vehicle i) and downstream (vehicle j) locations. This prior probability is formulated by explicitly considering the lane changing behaviors of vehicles and their arrival time probability at the downstream location.

Having obtained the probabilities of each upstream vehicle matching its feasible matches (P_{ij}), the optimal matching (i.e., V-ReID) is realized by solving a maximization problem on the constructed bipartite graph:

$$\max \ \sum_{\forall i \in U} \sum_{\forall j \in D} P_{ij} \delta_{ij} \tag{9}$$

$$\text{s.t.} \quad \delta_{ij} \in \{0,1\}, \forall i \in U, \forall j \in S(i) \tag{10}$$

$$\sum_{\forall j \in D} \delta_{ij} \leq 1, \forall i \in U \tag{11}$$

$$\sum_{\forall i \in U} \delta_{ij} \leq 1, \forall j \in D \tag{12}$$

Equation (9) is the objective of the optimization problem that aims to maximize the total matching probability. Equation (10) indicates the decision variables as binary integers. Equation (11) ensures that any upstream vehicle i can only be matched with at most one downstream vehicle, whereas Equation (12) ensures that any downstream vehicle j can only be matched with at most one upstream vehicle. This bipartite graph matching problem can be solved efficiently using a well-developed algorithm proposed by Galil (1986).

3.5 Step 5: Estimation of the lane-based travel time distributions by vehicle type

Using the V-ReID results from Step 4 (i.e., $\delta_{ij} = 1$ or 0), travel time samples for each matched pair of vehicles i and j (T_{ij}) are defined as

$$T_{ij} = \tau_j^D - \tau_i^U, \quad \text{if } \delta_{ij} = 1 \tag{13}$$

Note that the above T_{ij} is one of the travel time samples for these vehicles (i and j at upstream and downstream locations respectively) by vehicle type, which is classified in Step 2. The above T_{ij} is also one of the travel time samples in a particular lane, which

is based on the lane location of the matched vehicle at the upstream section. Travel time samples are then aggregated by lane and by vehicle type to generate the corresponding travel time distributions. The travel time distributions reflect the variation of travel times for a certain vehicle type from a given lane at the upstream section to the downstream section.

4. Results and discussion

The accuracy of the proposed method for lane-based travel time estimation by vehicle type is examined by conducting a case study having different lane markings for different lanes of a congested urban road in Hong Kong. The vehicle type classification accuracy, vehicle re-identification accuracy, and accuracy of the estimation of travel time distributions, means, and standard deviations are described and discussed in the following.

A cutting-edge existing method (Wang et al., 2014) using the same low-resolution video images is implemented for comparative analysis. This existing method adopted the same travel time window for re-identification of vehicles travelling in different lanes. Also, the existing method did not specifically consider appreciable differences of travel times in different lanes for different types of vehicles, which implied that different types of vehicles in different lanes have the same travel time estimation in their method.

4.1 Test site

The experiment of this case study is conducted on a four-lane urban road in Hong Kong (Chatham Road South, Westbound, Figure 4a). The lane markings of different lanes in this selected road segment are shown in Figure 2. It is seen that vehicles in Lane 1 are allowed to change lane to their right (Lane 2) in the upstream section but they are not allowed to change lane in the downstream section. Vehicles in Lane 2 are only allowed to change lane to their right (Lane 3) in the upstream section but are allowed to change

lane both to the left (Lane 1) and right (Lane 3) in the downstream section. Vehicles in Lane 3 are allowed to change lane to both their left (Lane 2) and right (Lane 4) in both upstream and downstream sections. Vehicles in Lane 4 are allowed to change lane to their left (Lane 3) in the upstream section but they are not allowed to change lane in the downstream section. In addition, the exit of the far-side lane (Lane 4) at the selected site leads to a flyover connecting to a major urban expressway for traffic traveling between urban areas in the east and west of Kowloon Peninsula in Hong Kong.

Two video cameras are installed on a footbridge that spans the selected road and connects the Innovation Tower and Block Z building of The Hong Kong Polytechnic University (Figure 4b). As shown in Figure 2, one of the cameras captures the upstream vehicles from the front whereas the other camera captures the downstream vehicles from the back.

{Insert Figure 4 here}

In this case study, the recorded videos have a resolution of 1920 × 1080 pixels and a frame rate of 25 frames per second. However, the camera views at the upstream and downstream locations are set to capture the whole four-lane section of the selected road. As a result, the image size/resolution of each identified vehicle is small (around 140 × 140 pixels). The license plate numbers of vehicles cannot be identified from these low-resolution video images.

The proposed method of estimating the travel time is implemented using data collected during a Wednesday morning peak hour (i.e., 8:00 to 9:00 a.m. on January 8, 2020). The results of the proposed method are compared against the ground truth obtained from the manual labeling of vehicle types and manual matching of the same vehicles for all vehicles in the peak hour. The proposed method is also compared with the existing method (Wang et al., 2014) using the same low-resolution video images.

4.2 Sample size

Manual matching and the removal of outliers (i.e., samples with a travel time longer than the 99.5th percentile or shorter than the 0.5th percentile) give 1996 pairs of matched samples within the study period. These samples are firstly classified into the six vehicle classes (sub-types): sedans, taxis, vans, minibuses, buses, and trucks. This classification is adopted in the discussion of the accuracies of vehicle type classification (sub-section 4.3) and vehicle re-identification (sub-section 4.4).

Table 3 shows the actual sample sizes by lane and by vehicle class. It is revealed that sedans have the largest proportion (52.1%) while minibuses have the smallest proportion (2.4%) among the six classes of vehicle. Empirical studies have found that the travelling speeds of small passenger cars (e.g. sedans and taxis) are distinctive from those of light commercial vehicles (e.g. vans and minibuses) and heavy commercial vehicles (e.g. buses, and trucks), while light and heavy commercial vehicles have similar travelling speeds (Chathoth & Asaithambi, 2018; Sil et al., 2020). The six vehicle classes are thus grouped into two vehicle types—small (sedans and taxis) and other (vans, minibuses, buses, and trucks) vehicles—for the analysis of travel time estimations in sub-sections 4.5 to 4.7.

{Insert Table 3 here}

To ensure sufficient samples for an objective representation of the lane-based travel time distribution by vehicle type, the required sample size n_{min} (Ernst et al., 2014; Yun & Qin, 2019) is determined as

$$n_{min} > \left(\frac{z_{\alpha/2} \cdot \sigma}{\varepsilon \cdot \mu}\right)^2 \quad (14)$$

where $z_{\alpha/2} = 1.645$ is the z-statistic for a confidence level of $1 - \alpha$ = 90%, ε is the permitted error percentage of the mean and is set as 10% in this case study, μ is the mean travel time, and σ is the standard deviation of the mean.

With the mean travel time (μ) and standard deviation of the mean (σ) for each lane and vehicle type obtained from manual matching, the required sample size by lane and by vehicle type is found using Equation (14). A comparison of actual and required sample sizes in Table 4 shows that there are sufficient samples for each vehicle type (i.e., small and other vehicles) in each lane.

{Insert Table 4 here}

4.3 Accuracy of vehicle type classification

In this study, the accuracy of vehicle type classification (ACC_t) is defined by

$$Acc_t = \frac{N_c^t}{N_{all}^t} \times 100\% \quad (15)$$

where N_{all}^t is the total number of identified vehicles and N_c^t is the number of vehicles with their vehicle classes correctly classified. As discussed in sub-section 3.2, a training data set is used to calibrate the number of template images (N_{tem}) and the fusion weight (w). In this experiment, it is found that $N_{tem} = 8$ and $w = 0.11$ give the maximum Acc_t in the training data set.

With the calibrated N_{tem} and w, the proposed vehicle type classification (Step 2) is carried out. Table 5 presents the confusion matrix of the six-vehicle-class classification. Each row in the table shows the distribution of estimated vehicle classes (resulted from Step 2) for that class of vehicle (ground truth). For example, the percentage 3.4% in the first row of Table 5 indicates that 3.4% of sedans are wrongly classified as taxis when using the proposed method (Step 2). The proposed classification method is

generally accurate as the classification accuracies range from 78.3% to 100% for different vehicle classes. Among the six vehicle classes, the classifications of taxis and buses are completely successful (100%) as taxis are distinct from other vehicle classes by color (i.e., taxis are red in urban areas of Hong Kong) while buses are relatively distinct in terms of their size. Compared with those two vehicle classes, sedans (78.3%) and trucks (80.0%) have low accuracies owing to their wide ranges of size and color. When all six vehicle classes are grouped together, the overall accuracy for the proposed classification approach is 85.6%. This vehicle type classification was not considered in the existing method (Wang et al., 2014).

{Insert Table 5 here}

4.4 Vehicle re-identification accuracy

Besides the classification accuracy, the accuracy of vehicle re-identification (vehicle matching) between the upstream and downstream locations is considered and analyzed. In this study, the vehicle re-identification accuracy (ACC_m) is defined by

$$ACC_m = \frac{N_c^m}{N_{all}^m - N_{null}^m} \times 100\% \quad (16)$$

where N_{all}^m is the total number of vehicles in the upstream section, N_{null}^m is the number of vehicles that are not re-identified with any downstream vehicle, and N_c^m is the number of vehicles that are correctly re-identified. The re-identification accuracies of the proposed and the existing methods are respectively provided in Tables 6a and 6b.

Table 6a gives the accuracy of the proposed V-ReID for each of the six vehicle classes and each of the four traffic lanes. As expected, re-identifying the same vehicle in the upstream and downstream locations is more difficult than classifying the vehicles into correct vehicle classes. Thus, the re-identification accuracy of the proposed method

(Table 6a) is generally lower than the classification accuracy (Table 5). Despite the difficulties of V-ReID, 52.4% of vehicles are correctly re-identified, which provides accurate travel time data for the estimation of the travel time distribution by lane and vehicle type.

The re-identification accuracy (all lanes) ranges from 42.4% to 81.2% for the six vehicle classes. Table 6a reveals that vehicle classes with larger size (i.e., trucks and buses) generally have a higher re-identification accuracy (62.5%–81.2%) than vehicle classes with smaller size (i.e., sedans, taxis, and vans; re-identification accuracy ranging 42.4%–59.8%). The reason for such a difference is that larger vehicles are more distinct in appearance and thus have greater probability of a correct match (Equation 8). Minibuses, which are a type of public transportation mode in Hong Kong, have high re-identification accuracy (70.2%) owing to their unique shape and color despite being of similar size to vans.

A comparison of the V-ReID accuracy among different lanes reveals that the accuracy for Lane 4 is generally lower than the accuracies for the other lanes. This can be explained by the highly varied travel time distributions of this lane (see Figure 5a), which result in a larger travel time window (Equations 5 and 6). The larger travel time window can include more vehicles as feasible matches (Equation 7) but also increases the chance of incorrect matching, which lowers the re-identification accuracy.

Compared to the proposed method, the existing method has lower V-ReID accuracy in general (37.3%). For deeper analysis, Table 6b provides the V-ReID accuracy by lane and by vehicle class, despite that the existing method neither identified vehicles' lane locations nor classified vehicle types. The V-ReID accuracies are especially low for Lane 4, ranging from 2.1% to 27.3% for the six vehicle classes. The reason is that the existing method used the same travel time window for different lanes, while travel times

in Lane 4 are much longer than other lanes. As a result, many correct matches are not included by the travel time window of the existing method.

{Insert Table 6 here}

In general, the proposed V-ReID outperforms the existing method due to more accurate lane-based travel time windows. Since the proposed method explicitly considers differences of travel times among lanes, the travel time variations and the travel time windows for each lane are obviously smaller than those for all vehicles. More invalid vehicle matches are thus screened out by the proposed method to improve the V-ReID accuracies.

4.5 Travel time distribution

For each pair of re-identified vehicles, including both correct and incorrect matches, travel time samples are estimated using Equation (13). Grouping these travel time samples for different vehicle types and lanes, the corresponding travel time distributions can be estimated. As previously discussed, the six vehicle classes are grouped into two vehicle types (i.e., small vehicles and other vehicles) to provide sufficient samples for the analysis of travel times. Figure 5a shows the ground truth of travel time distributions by the four lanes and two vehicle types for the study period (8:00 to 9:00 a.m. on Wednesday January 8, 2020). Figures 5b and 5c respectively present the travel time distributions estimated by the proposed and existing methods. Each of the histograms shown in Figure 5 has a bin width of 15 seconds. The figure reveals that the travel time distributions vary by lane and vehicle type.

{Insert Figure 5 here}

The ground truth of travel time distributions (Figure 5a) reveals that the travel times (for small vehicles and other vehicles) in Lane 1 are the least varied among the lanes. This low variation is due to traffic being prevented from merging into Lane 1 by

the lane markings between Lanes 1 and 2 in the upstream section and non-overlapping area (see Figure 2 and the ground truth demands from other lanes to Lane 1 in Table 10a). As a result, traffic in Lane 1 is less disrupted and can maintain uniform travel times. In Figure 5a, the ground-truth travel time distributions for Lane 3 are relatively long and more spread-out than those for Lane 2. This result is due to traffic in Lane 3 being allowed to change to Lanes 2 and 4 whereas traffic in Lane 2 is only allowed to change to Lane 3 in the upstream section and the non-overlapping area (see lane markings in Figure 2). Thus, there is potentially more lane-changing traffic in Lane 3 (see ground truth demands from Lane 3 in Table 10a), which generally has a longer travel time than Lane 2 (see ground truth mean travel times in Table 9), and the traffic staying in Lane 3 has a higher chance of being affected by the lane-changing vehicles. As a result, travel times for Lane 3 are longer and more varied than those for Lane 2. Additionally, as Lane 4 is relatively congested (see the longer and more spread-out travel time distribution in Figure 5a), it takes more time for vehicles to leave Lane 3 and merge into Lane 4. Thus, the impact of traffic merging into Lane 4 is larger than that for the other lanes and leads to a more spread-out travel time of Lane 3 than that of Lane 2. The ground-truth travel times of Lane 4 (Figure 5a) are much longer than those of the other three lanes and follow a different distribution. This result can be explained by the fact that the downstream of Lane 4 is connected to a major urban expressway. Congestion on this major urban expressway propagates back and substantially increases the mean and variance of travel times in Lane 4. The above comparisons and discussions of the travel time distributions of different lanes reveal that travel times increase and become more varied with the presence/increase of lane-changing traffic. In other words, the design of lane markings, which governs the possibilities of lane changing, affects the travel times within a section and is thus worthy of further investigation.

The Hellinger distance (HD) (Prokhorchuk et al., 2020; Yun & Qin, 2019) is adopted to measure the distances/dis-similarities between the estimated travel time distributions (Figures 5b and 5c) and the ground truth (Figure 5a):

$$HD = \frac{1}{\sqrt{2}}\sqrt{\sum_{i=1}^{n}\left(\sqrt{\overline{Y}_i} - \sqrt{Y_i}\right)^2} \quad (17)$$

where n is the number of bins of the travel time histogram, i is the index of the bin, and $\overline{Y}_i$ and Y_i are respectively the probability (or relative frequency) of the true and estimated travel times in bin i. The value of HD ranges from 0 to 1, where HD = 0 indicates that two distributions are the same and HD = 1 represents no similarity between two distributions. Therefore, the less the HD, the higher accuracy is the estimated distribution. Using Equation (17), the HDs of each pair of histograms for ground truth and estimated travel times (Figure 5) are calculated. The results of the proposed and existing methods are respectively shown in Tables 7a and 7b.

Table 7a shows that the travel time distributions estimated by the proposed method are generally accurate, with the HDs being less than 0.189 for all vehicle types and lanes. The maximum distance of 0.189 occurs for other vehicles (i.e., vans, minibuses, buses, and trucks) traveling in Lane 3. On average, the HD by lane and by vehicle type is 0.137 for the proposed method (the average of the first four rows of Table 7a). The HDs in the last row of Table 7a represent general estimation accuracy for the two vehicle types. The small and other vehicles respectively have HDs of 0.079 and 0.052, which reflects high accuracy of the estimations.

Table 7b shows that the estimations of travel time distributions are less accurate by the existing method. The HD by lane and by vehicle type is averagely 0.321 (the average of the first four rows of Table 7b), which are 2.3 times as large as that of the proposed method. This can be attributed to the implicit assumption that different types of

vehicles in different lanes have the same travel time distribution. As shown in Figure 5c, the same estimations of travel time distributions are generally close to the ground truth for Lanes 1 and 2, with the HDs being less than 0.184. However, the estimation errors are larger for more congested lanes, especially for Lane 4, where the HDs are respectively 0.746 and 0.738 for small and other vehicle types.

{Insert Table 7 here}

Compared to the existing method, the proposed method has higher V-ReID accuracy and thus more valid samples can be collected for the estimations of travel time distributions, including travel time samples for Lane 4, i.e. the relatively congested lane. Also, the proposed method distinguishes these travel time samples by vehicle types and by lane locations, and therefore differences of travel times among vehicle types and lanes are reflected and the estimations of travel time distributions are more detailed and more accurate.

4.6 Means of travel times

Using travel time samples of re-identified vehicles for different lanes and vehicle types, the means of travel times are estimated and the corresponding accuracy is evaluated. Table 8a shows the estimated mean travel times of the proposed method. The absolute percentage errors, as compared with the ground truth, range from 0.1% to 4.1%. The mean travel times estimated for Lanes 3 and 4 generally have larger errors (2.8%–4.1%) than those estimated for Lanes 1 and 2 (0.1%–3.7%). This can be explained by the fact that congestion in Lane 4, which is due to the bottleneck at the exit, and more lane-changing maneuvers in Lane 3 lead to longer and more varied travel times (Figure 5). The congestion and maneuvers result in longer travel time windows (Equations 5 and 6) for Lanes 3 and 4 and lower corresponding V-ReID accuracy. As a result, travel time samples for Lanes 3 and 4 include more noise from incorrect matching.

The mean estimations of travel times resulted from the proposed method are more accurate than those from the existing method. As shown in Table 8b, the existing method adopted the same mean estimation for all vehicles, which leads to large estimation errors. Take Lane 4 for example, the absolute percentage errors reach 77.5% and 78.2% for two types of vehicles. The absolute percentage errors for small and other vehicle types in all lanes are also not accurate, respectively 44.2% and 46.6%. In contrast, the proposed method collects more valid travel time samples and divides these samples by vehicle type and by lane for mean estimations. Similar to the estimations of travel time distributions, the mean estimations of the proposed method are more accurate.

{Insert Table 8 here}

Table 8a reveals that the estimated mean travel times increase from Lane 1 to Lane 4, which confirms the observations in Figure 5 and can be explained by the reasons relating to lane markings and downstream congestion discussed in sub-section 4.5. A comparison of the estimated mean travel times of different vehicle types (Table 8a) reveals that the small vehicles generally have smaller errors (2.3%) than the other vehicles (3.9%). In terms of the estimated mean travel times, as expected, the small vehicles have shorter travel times than the other vehicles in all lanes, except for Lane 3. In Lane 3, the estimated mean travel time of the small vehicles is 22.8 seconds, which is longer than that of the other vehicles (19.7 seconds).

The mean travel times obtained from the manual matching (i.e., the ground truth) of the small and other vehicles between lanes (Table 9) are further investigated to explain this unexpected result for different vehicle types. A comparison of Tables 9a and 9b reveals that the small vehicles have shorter travel times than the other vehicles in most cases. Among vehicles that do not change lane (i.e., the diagonal values in Table 9a and 9b), the travel times of the small vehicles in Lanes 1, 2, 3, and 4 are respectively 8.8, 10.9,

25.1, and 57.2 seconds, all of which are shorter than the corresponding times for the other vehicles (i.e., 9.1, 12.7, 27.0, and 58.6 seconds respectively). In the definition of vehicle types (sub-section 4.2), the small vehicles (sedans and taxis) are passenger cars while the other vehicles (vans, minibuses, buses, and trucks) are heavy vehicles. Many empirical studies have found that heavy vehicles travel at lower speeds and have longer travel times because of their limited maneuverability, such as their limited acceleration and deceleration (Cao et al., 2016; Moridpour et al., 2015), and they improve their fuel economy by traveling at lower speed (Zhou et al., 2018). Thus, the observed longer travel times of the other vehicles, as compared with the small vehicles, are consistent with the empirical findings in the literature in the case that there is no lane changing (i.e., the diagonal values in Table 9b).

Nevertheless, when there is lane changing between the upstream and downstream sections (i.e., the off-diagonal values in Tables 9a and 9b), there are cases in which small vehicles have longer travel times (e.g., vehicles traveling from Lane 2 upstream to Lane 4 downstream). The travel times of these lane-changing vehicles comprise the duration of travel in the lanes and the duration of lane-changings. Previous studies have used empirical data to reveal that in some cases heavy vehicles may take less time than small vehicles (Aghabayk et al., 2011; Toledo & Zohar, 2007).

The shorter lane-changing duration of heavy vehicles can be explained by the lane-changing behaviors and characteristics of the heavy vehicles. Under heavy traffic conditions, drivers change lane either through the courteous yielding of the following vehicle or by forcing the following vehicle to slow down (Yang et al., 2019). For the following vehicles, the analysis of naturalistic driving data has shown that some drivers of the following vehicle brake urgently to yield to the lane-changing vehicle and avoid a collision (Wang et al., 2019). Heavy vehicles, owing to their large size and weight,

impose both physical and psychological effects on surrounding vehicles (Moridpour et al., 2015). Additionally, owing to the lower maneuverability of heavy vehicles, empirical data show that they maintain a more constant speed during the lane-changing maneuver than small vehicles do (Aghabayk et al., 2011; Moridpour et al., 2010). Thus, owing to the physical/psychological effect and low maneuverability of heavy vehicles, the following vehicles will be more cautious in responding to the lane-changing of heavy vehicles and yield to the heavy vehicles because of safety concerns (Toledo & Zohar, 2007). As a result, it could be easier for heavy vehicles to change lanes, which would shorten their lane-changing duration. In addition, drivers of the other vehicles (i.e., vans, minibuses, buses, and trucks) are usually professional drivers with more experience in lane-changing, especially when there is congestion, and they will therefore have a shorter lane-changing duration (Aghabayk et al., 2011; Toledo & Zohar, 2007). The above explains that it is possible for the small vehicles to have longer travel times than other vehicles, when there are lane-changing maneuvers between the upstream and downstream sections (i.e., the off-diagonal values in Tables 9a and 9b).

{Insert Table 9 here}

The mean travel time of each lane (the last columns in Tables 9a and 9b) is the weighted average of travel times to all downstream lanes with the weight taken as the corresponding vehicle proportion. Tables 10a and 10b respectively give the number, and proportion in brackets, of the small and other vehicles for different lanes from manual matching (i.e., ground truth). Despite the small vehicles having shorter travel times when traveling from Lane 3 (upstream) to Lane 3 (downstream) (Tables 9a and 9b), their proportion (35.5% for the small vehicles and 30.5% for the other vehicles) is not sufficient to outweigh the long travel times (see Table 9a and 9b for Lane 3 to Lane 2 and Lane 3 to Lane 4) of lane-changing vehicles (with a proportion of 64.5% for small vehicles and

69.5% for other vehicles). Thus, in Table 9, the ground-truth travel time of the small vehicles in Lane 3 (23.8 seconds), which is the weighted average of all maneuvers, is longer than that of the other vehicles (20.5 seconds). These findings of ground-truth travel times for Lane 3 suggest that the proposed travel time estimations for the small and other vehicles in Lane 3 (Table 8a) are reasonable.

{Insert Table 10 here}

4.7 Standard deviations of travel times

The standard deviation of travel times is estimated using travel time samples of re-identified vehicles for different lanes and vehicle types. The results of the proposed and existing methods are respectively shown in Tables 11a and 11b. Table 11a reveals that the standard deviations of travel times estimated by the proposed method increase from Lane 1 to Lane 4. This can be explained by lane markings and downstream congestion as discussed in sub-section 4.5. As expected, the errors of standard deviation estimation are generally larger than those of the mean estimation but still fall in an acceptable range with a maximum error of 10.7%. The aggregated estimation errors of each vehicle type (i.e., the last row of Table 11a) are less than 4.3%.

The proposed method outperforms the existing method in the estimations of standard deviation, similar to the estimations of travel time distributions and mean travel times. As previously discussed, more travel time samples are obtained by the proposed method due to its higher V-ReID accuracy. In contrast, the existing method collect limited samples especially in Lane 4 where travel time distributions varied most highly (see Figure 5a). Consequently, the standard deviations estimated by the existing method are smaller than those resulted from the proposed method.

{Insert Table 11 here}

5. Conclusions and future research

This paper proposes a lane-based V-ReID and travel time estimation framework by vehicle type for congested urban roads with lane-changing maneuvers. Lanes of the same road segment can have distinct lane-changing conditions, and differences in travel times between different vehicle types and different traffic lanes were thus investigated. The proposed method enhances the V-ReID accuracy, and therefore more travel time samples are collected for the accurate estimation of travel time distributions by lane and by vehicle type. These information can be very helpful for various traffic management purposes such as determining the entry and exit locations of bus-only lane; changing lane markings for controlling the merging/diverging of different vehicles; and estimating the traffic emission/fuel consumption by vehicle types etc.

A four-lane urban road with different lane markings for different lanes in Hong Kong was taken as a test site for a case study. The proposed method was implemented in the case study to estimate travel times by vehicle type and traffic lane. A cutting-edge existing method using the same low-resolution video images was also implemented for comparative analysis. Results showed that the proposed method outperforms the existing method and the estimation results are generally accurate. The classification accuracies ranged from 78.3% for sedans to 100% for taxis and buses. The V-ReID accuracies ranged from 42.4% for sedans to 81.2% for buses. Larger vehicles (e.g., buses and trucks) had a higher re-identification accuracy. In the estimation of travel time distributions, it was found that the Hellinger distances between the estimated travel time distributions and the ground truth are less than 0.189 for all vehicle types and lanes. The average of Hellinger distances is 0.137, which is 57% less than that of the existing method. The errors of the corresponding mean estimates ranged from 0.1% for the other vehicles in Lane 1 to 4.1% for the small vehicles in Lane 3. The errors of the standard deviation

estimates ranged from 1.6% for the other vehicles in Lane 4 to 10.7% for the other vehicles in Lane 2. It was shown in this case study that the estimation errors of the travel time distributions are varied by lane and vehicle type on the four-lane road segment with different lane-changing maneuvers.

In future work, the proposed V-ReID can be extended to road segments of longer distance for travel time estimation. More spatial-temporal information, such as the vehicle sequence, can be considered to filter out invalid vehicles for a road segment with many entries/exits. On a congested road segment, there are far fewer discretionary lane-changing maneuvers. The vehicle sequence of each traffic lane should remain stable, except that some vehicles enter their target lanes or exit their initial lanes because of mandatory lane changing. For example, if a downstream vehicle cannot be matched to an upstream vehicle with similar leading and following vehicles, this vehicle probably enters in the middle of the road segment and thus should be filtered out. Additionally, in view of low-resolution video images having different angles of view, it would be worthwhile to make use of more vehicle appearance information, such as the roof patterns, side views, and/or advertisements of the vehicles, in improving the quality of V-ReID. Moreover, since video images are sensitive to low illumination conditions (e.g. adverse weather), further studies are required to extend the proposed V-ReID method by using other data sources such as thermal images and axle-weight measurements (Basar et al., 2018; Li et al., 2020). Heterogeneous data fusion is encouraged to enhance the robustness of V-ReID.

As for the investigation of lane-changing effects and travel time distributions, this case study revealed that the travel times of different vehicle types varied according to the traffic lanes, the lane markings of which differed in, for example, their locations and lengths. In the field of urban road design and/or traffic management, the effect of lane markings, which govern the possibility of lane changing, on travel time distributions

should be further investigated to balance the efficiency and flexibility of the urban road design. Moreover, the effects of vehicle types on the lane-changing duration and thus the lane-based travel time deserve further studies. The effects of various factors, such as the traffic density, traffic signal timing, and relative speed of the lane-changing vehicle, on lane-changing behaviors and duration are also worthy of further investigation. To observe and model lane-changing effects in a more detailed and fine-grained manner, vehicle trajectory data should be collected and analyzed. Last but not least, the integration of model-based and data-driven approaches can be further investigated to improve the estimation of the travel time distribution by vehicle type for the entire road network in practice.

Acknowledgments

This work was supported by the Research Grants Council of the Hong Kong Special Administrative Region, China under Grants PolyU R5029-18, HKU R7027-18 and 17204919; and the Research Institute for Sustainable Urban Development of the Hong Kong Polytechnic University under Grant 5-ZJM5. The fifth author was supported by the Francis S Y Bong Endowed Professorship in Engineering.

Disclosure statement

No potential conflict of interest was reported by the author(s).

References

Aghabayk, K., Moridpour, S., Young, W., Sarvi, M., & Wang, Y. B. (2011). Comparing heavy vehicle and passenger car lane-changing maneuvers on arterial roads and freeways. *Transportation Research Record*, *2260*(1), 94-101. https://doi.org/10.3141/2260-11

Araghi, B. N., Krishnan, R., & Lahrmann, H. (2016). Mode-specific travel time estimation using bluetooth technology. *Journal of Intelligent Transportation Systems*, *20*(3), 219-228. https://doi.org/10.1080/15472450.2015.1052906

Bai, Y., Lou, Y., Gao, F., Wang, S., Wu, Y., & Duan, L.-Y. (2018). Group-sensitive triplet embedding for vehicle reidentification. *IEEE Transactions on Multimedia*, *20*(9), 2385-2399. https://doi.org/10.1109/tmm.2018.2796240

Basar, G., Cetin, M., & Nichols, A. P. (2018). Comparison of vehicle re-identification models for trucks based on axle spacing measurements. *Journal of Intelligent Transportation Systems*, *22*(6), 517-529. https://doi.org/10.1080/15472450.2018.1441027

Cao, X., Young, W., Sarvi, M., & Kim, I. (2016). Study of mandatory lane change execution behavior model for heavy vehicles and passenger cars. *Transportation Research Record*, *2561*(1), 73-80. https://doi.org/10.3141/2561-09

Celikoglu, H. B. (2013). Flow-based freeway travel-time estimation: A comparative evaluation within dynamic path loading. *IEEE Transactions on Intelligent Transportation Systems*, *14*(2), 772-781. https://doi.org/10.1109/tits.2012.2234455

Chathoth, V., & Asaithambi, G. (2018). Modeling Free-flow Speeds on Undivided Roads in Mixed Traffic with Weak Lane Discipline. *Transportation Research Record*, *2672*(15), 105-117. https://doi.org/10.1177/0361198118794538

Chen, B. Y., Li, Q., & Lam, W. H. K. (2016). Finding the k reliable shortest paths under travel time uncertainty. *Transportation Research Part B: Methodological*, *94*, 189-203. https://doi.org/10.1016/j.trb.2016.09.013

Chen, P., Zeng, W., Chen, M., Yu, G., & Wang, Y. (2018). Modeling arterial travel time distribution by accounting for link correlations: a copula-based approach. *Journal of Intelligent Transportation Systems,* *23*(1), 28-40. https://doi.org/10.1080/15472450.2018.1484738

Chiou, J. M., Liou, H. T., & Chen, W. H. (2021). Modeling Time-Varying Variability and Reliability of Freeway Travel Time Using Functional Principal Component Analysis. *IEEE Transactions on Intelligent Transportation Systems, 22*(1), 257-266. https://doi.org/10.1109/tits.2019.2956090

Coifman, B., & Cassidy, M. (2002). Vehicle reidentification and travel time measurement on congested freeways. *Transportation Research Part A: Policy and Practice*, *36*(10), 899-917. https://doi.org/10.1016/S0965-8564(01)00046-5

Duan, P., Mao, G., Kang, J., & Huang, B. (2020). Estimation of Link Travel Time Distribution with Limited Traffic Detectors. *IEEE Transactions on Intelligent Transportation Systems,* *21*(9), 3730-3743. https://doi.org/10.1109/tits.2019.2932053

Ernst, J. M., Krogmeier, J. V., & Bullock, D. M. (2014). Estimating required probe vehicle re-identification requirements for characterizing link travel times. *IEEE Intelligent Transportation Systems Magazine*, *6*(1), 50-58. https://doi.org/10.1109/mits.2013.2288648

Filipovska, M., Mahmassani, H. S., & Mittal, A. (2021). Estimation of Path Travel Time Distributions in Stochastic Time-Varying Networks with Correlations. *Transportation Research Record,* *2675*(11), 498-508.

https://doi.org/10.1177/03611981211018464
Fu, F., Qian, W., & Dong, H. (2019). Estimation of Route Travel Time Distribution with Information Fusion from Automatic Number Plate Recognition Data. *Journal of Transportation Engineering, Part A: Systems, 145*(7), 04019029. https://doi.org/10.1061/jtepbs.0000242
Galil, Z. (1986). Efficient algorithms for finding maximum matching in graphs. *ACM Computing Surveys*, *18*(1), 23-38. https://doi.org/10.1145/6462.6502
Guo, Y., & Yang, L. (2020). Reliable Estimation of Urban Link Travel Time Using Multi-Sensor Data Fusion. *Information, 11*(5), 267. https://doi.org/10.3390/info11050267
Huang, G., Liu, Z., Van Der Maaten, L., & Weinberger, K. Q. (2017). Densely connected convolutional networks. *2017 IEEE Conference on Computer Vision and Pattern Recognition (CVPR)*, 2261-2269. https://doi.org/10.1109/CVPR.2017.243
Jenelius, E., & Koutsopoulos, H. N. (2013). Travel time estimation for urban road networks using low frequency probe vehicle data. *Transportation Research Part B: Methodological*, *53*(1), 64-81. https://doi.org/10.1016/j.trb.2013.03.008
Jiang, Z., Chen, X., & Ouyang, Y. (2017). Traffic state and emission estimation for urban expressways based on heterogeneous data. *Transportation Research Part D: Transport and Environment*, *53*(1), 440-453. https://doi.org/10.1016/j.trd.2017.04.042
Khan, S. D., & Ullah, H. (2019). A survey of advances in vision-based vehicle re-identification. *Computer Vision and Image Understanding*, *182*(1), 50-63. https://doi.org/10.1016/j.cviu.2019.03.001
Kwong, K., Kavaler, R., Rajagopal, R., & Varaiya, P. (2009). Arterial travel time estimation based on vehicle re-identification using wireless magnetic sensors. *Transportation Research Part C: Emerging Technologies*, *17*(6), 586-606. https://doi.org/10.1016/j.trc.2009.04.003
Li, H., Li, C., Zhu, X., Zheng, A., & Luo, B. (2020). Multi-Spectral Vehicle Re-Identification: A Challenge. *Proceedings of the AAAI Conference on Artificial Intelligence*, *34*(7), 11345-11353. https://doi.org/10.1609/aaai.v34i07.6796
Li, M., Chen, X., & Ni, W. (2016). An extended generalized filter algorithm for urban expressway traffic time estimation based on heterogeneous data. *Journal of Intelligent Transportation Systems*, *20*(5), 474-484. https://doi.org/10.1080/15472450.2016.1153426
Li, R., Rose, G., & Sarvi, M. (2006). Evaluation of speed-based travel time estimation models. *Journal of Transportation Engineering*, *132*(7), 540-547. https://doi.org/10.1061/(ASCE)0733-947X(2006)132:7(540)
Lu, L., He, Z., Wang, J., Chen, J., & Wang, W. (2021). Estimation of lane-level travel time distributions under a connected environment. *Journal of Intelligent Transportation Systems*, *25*(5), 501-512. https://doi.org/10.1080/15472450.2020.1854093
Ma, Z., Koutsopoulos, H. N., Ferreira, L., & Mesbah, M. (2017). Estimation of trip travel time distribution using a generalized Markov chain approach. *Transportation Research Part C: Emerging Technologies, 74*(1), 1-21. https://doi.org/10.1016/j.trc.2016.11.008
Mori, U., Mendiburu, A., Álvarez, M., & Lozano, J. A. (2015). A review of travel time estimation and forecasting for advanced traveller information systems. *Transportmetrica A*, *11*(2), 119-157. https://doi.org/10.1080/23249935.2014.932469
Moridpour, S., Mazloumi, E., & Mesbah, M. (2015). Impact of heavy vehicles on

surrounding traffic characteristics. *Journal of Advanced Transportation*, *49*(4), 535-552. https://doi.org/10.1002/atr.1286

Moridpour, S., Sarvi, M., & Rose, G. (2010). Modeling the lane-changing execution of multiclass vehicles under heavy traffic conditions. *Transportation Research Record*, *2161*(1), 11-19. https://doi.org/10.3141/2161-02

Oliveira-Neto, F. M., Han, L. D., & Jeong, M. K. (2012). Online license plate matching procedures using license-plate recognition machines and new weighted edit distance. *Transportation Research Part C: Emerging Technologies*, *21*(1), 306-320. https://doi.org/10.1016/j.trc.2011.11.003

Prokhorchuk, A., Dauwels, J., & Jaillet, P. (2020). Estimating travel time distributions by Bayesian network inference. *IEEE Transactions on Intelligent Transportation Systems*, *21*(5), 1867-1876. https://doi.org/10.1109/tits.2019.2899906

Redmon, J., & Farhadi, A. (2018). YOLOv3: An incremental improvement. *ArXiv:1804.02767*. Retrieved March 30, 2021, from http://arxiv.org/abs/1804.02767

Samara, A., Rempe, F., & Gottlich, S. (2021). A novel approach for vehicle travel time distribution: copula-based dependent discrete convolution. *Transportation Letters*, 1-12. https://doi.org/10.1080/19427867.2021.1941707

Sanaullah, I., Quddus, M., & Enoch, M. (2016). Developing travel time estimation methods using sparse GPS data. *Journal of Intelligent Transportation Systems*, *20*(6), 532-544. https://doi.org/10.1080/15472450.2016.1154764

Shi, C., Chen, B. Y., Lam, W. H. K., & Li, Q. (2017). Heterogeneous data fusion method to estimate travel time distributions in congested road networks. *Sensors*, *17*(12). 1-22. https://doi.org/10.3390/s17122822

Sil, G., Nama, S., Maji, A., & Maurya, A. K. (2020). Effect of horizontal curve geometry on vehicle speed distribution: a four-lane divided highway study. *Transportation Letters*, *12*(10), 713-722. https://doi.org/10.1080/19427867.2019.1695562

Soriguera, F., & Robusté, F. (2011). Estimation of traffic stream space mean speed from time aggregations of double loop detector data. *Transportation Research Part C: Emerging Technologies*, *19*(1), 115-129. https://doi.org/10.1016/j.trc.2010.04.004

Sumalee, A., Wang, J., Jedwanna, K., & Suwansawat, S. (2012). Probabilistic fusion of vehicle features for reidentification and travel time estimation using video image data. *Transportation Research Record*, *2308*(1), 73-82. https://doi.org/10.3141/2308-08

Sun, C. C., Arr, G. S., Ramachandran, R. P., & Ritchie, S. G. (2004). Vehicle reidentification using multidetector fusion. *IEEE Transactions on Intelligent Transportation Systems*, *5*(3), 155-164. https://doi.org/10.1109/tits.2004.833770

Tam, M. L., & Lam, W. H. K. (2011). Application of automatic vehicle identification technology for real-time journey time estimation. *Information Fusion*, *12*(1), 11-19. https://doi.org/10.1016/j.inffus.2010.01.002

Tang, J., Hu, J., Hao, W., Chen, X., & Qi, Y. (2020). Markov Chains based route travel time estimation considering link spatio-temporal correlation. *Physica A: Statistical Mechanics and its Applications, 545*, 123759. https://doi.org/10.1016/j.physa.2019.123759

Tang, K., Chen, S., Liu, Z., & Khattak, A. J. (2018). A tensor-based Bayesian probabilistic model for citywide personalized travel time estimation. *Transportation Research Part C: Emerging Technologies, 90*(1), 260-280. https://doi.org/10.1016/j.trc.2018.03.004

Tang, Z., Wang, G., Xiao, H., Zheng, A., & Hwang, J.-N. (2018). Single-camera and inter-camera vehicle tracking and 3D speed estimation based on fusion of visual and

semantic features. *Proceedings of the 2018 IEEE/CVF Conference on Computer Vision and Pattern Recognition Workshops (CVPRW)*, 108-115. https://doi.org/10.1109/CVPRW.2018.00022

Toledo, T., & Zohar, D. (2007). Modeling duration of lane changes. *Transportation Research Record*, *1999*(1), 71-78. https://doi.org/10.3141/1999-08

Uno, N., Kurauchi, F., Tamura, H., & Iida, Y. (2009). Using Bus Probe Data for Analysis of Travel Time Variability. *Journal of Intelligent Transportation Systems*, *13*(1), 2-15. https://doi.org/10.1080/15472450802644439

Wang, J., Indra-Payoong, N., Sumalee, A., & Panwai, S. (2014). Vehicle reidentification with self-adaptive time windows for real-time travel time estimation. *IEEE Transactions on Intelligent Transportation Systems*, *15*(2), 540-552. https://doi.org/10.1109/tits.2013.2282163

Wang, X., Yang, M., & Hurwitz, D. (2019). Analysis of cut-in behavior based on naturalistic driving data. *Accident Analysis and Prevention*, *124*(1), 127-137. https://doi.org/10.1016/j.aap.2019.01.006

Wojke, N., Bewley, A., & Paulus, D. (2017). Simple online and realtime tracking with a deep association metric. *Proceedings of the 2017 IEEE International Conference on Image Processing (ICIP)*, 3645-3649. https://doi.org/10.1109/ICIP.2017.8296962

Yang, M., Wang, X., & Quddus, M. (2019). Examining lane change gap acceptance, duration and impact using naturalistic driving data. *Transportation Research Part C: Emerging Technologies*, *104*(1), 317-331. https://doi.org/10.1016/j.trc.2019.05.024

Yang, Q., Wu, G., Boriboonsomsin, K., & Barth, M. (2017). A novel arterial travel time distribution estimation model and its application to energy/emissions estimation. *Journal of Intelligent Transportation Systems, 22*(4), 325-337. https://doi.org/10.1080/15472450.2017.1365606

Yu, W., Park, S., Kim, D. S., & Ko, S.-S. (2015). An Arterial Incident Detection Procedure Utilizing Real-Time Vehicle Reidentification Travel Time Data. *Journal of Intelligent Transportation Systems*, *19*(4), 370-384. https://doi.org/10.1080/15472450.2014.972762

Yun, M., & Qin, W. (2019). Minimum sampling size of floating cars for urban link travel time distribution estimation. *Transportation Research Record*, *2673*(3), 24-43. https://doi.org/10.1177/0361198119834297

Yun, M., Qin, W., Yang, X., & Liang, F. (2019). Estimation of urban route travel time distribution using Markov chains and pair-copula construction. *Transportmetrica B: Transport Dynamics, 7*(1), 1521-1552. https://doi.org/10.1080/21680566.2019.1637798

Zhang, C., Chen, B. Y., Lam, W. H. K., Ho, H. W., Shi, X., Yang, X., Ma, W., Wong, S. C., & Chow, A. H. F. (2021). Vehicle Re-identification for Lane-level Travel Time Estimations on Congested Urban Road Networks Using Video Images. *IEEE Transactions on Intelligent Transportation Systems*, 1-17. https://doi.org/10.1109/tits.2021.3118206

Zhang, K., Jia, N., Zheng, L., & Liu, Z. (2019). A novel generative adversarial network for estimation of trip travel time distribution with trajectory data. *Transportation Research Part C: Emerging Technologies, 108*(1), 223-244. https://doi.org/10.1016/j.trc.2019.09.019

Zheng, F., & Van Zuylen, H. (2014). The Development and Calibration of a Model for Urban Travel Time Distributions. *Journal of Intelligent Transportation Systems*, *18*(1), 81-94. https://doi.org/10.1080/15472450.2013.802155

Zhou, J., Rilett, L., Jones, E., & Chen, Y. (2018). Estimating passenger car equivalents on level freeway segments experiencing high truck percentages and differential average speeds. *Transportation Research Record*, *2672*(15), 44-54. https://doi.org/10.1177/0361198118798237

List of tables

Table 1. Summary of key studies on travel time estimation*

	Data sources	Real data	Travel time estimation			Study sites
			Overall	By lane	By vehicle type	
Li et al. (2006)	Loop detector data	√	Mean			Freeways
Tam & Lam (2011)	AVI data	√	Mean Std.			Urban roads
Wang et al. (2014)	Video images	√	Mean Std.			Freeways
Sanaullah et al. (2016)	GPS data	√	Mean			Freeways
Li et al. (2016)	Loop detector data and GPS data	√	Mean			Urban roads
Shi et al. (2017)	Video images and AVI data	√	Mean Std. Dist.			Urban roads
Ma et al. (2017)	AVI data	√	Mean Std. Dist.			Freeways and urban roads
Zhang et al. (2019)	GPS data	√	Mean Std. Dist.			Freeways and urban roads
Tang et al. (2020)	Microwave detector data	√	Mean Std. Dist.			Freeways
Lu et al. (2021)	Connected vehicle data		Mean Std. Dist.	Mean Std. Dist.		Urban roads
Zhang et al. (2021)	Video images from different angles of view	√	Mean Std. Dist.	Mean Std. Dist.		Urban roads
The proposed method	**Video images from different angles of view**	**√**	**Mean Std. Dist.**	**Mean Std. Dist.**	**Mean Std. Dist.**	**Urban roads**

*Std. = Standard deviation; Dist. = Distribution

Table 2. Distance measures between a given vehicle image and template images (an example)

Template images	 Sedan	 Taxi	 Van	 Minibus	 Bus	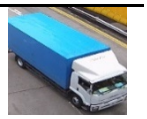 Truck
 Vehicle image	2.1207	1.9752	1.2851	0.9523	0.9679	**0.9241**

Table 3. Actual sample size by lane and by vehicle class

	Small		Other			
	Sedan	Taxi	Van	Minibus	Bus	Truck
Lane 1	236	19	32	9	57	37
Lane 2	354	147	64	23	91	55
Lane 3	293	129	39	11	56	48
Lane 4	157	39	28	5	6	61
All lanes	**1040**	334	163	**48**	210	201

Table 4. Actual and required sample size by lane and by vehicle type

	Small		Other	
	Actual	Required	Actual	Required
Lane 1	255	123	135	130
Lane 2	501	160	233	201
Lane 3	422	197	154	136
Lane 4	196	50	100	48
All lanes	1374	233	622	235

Table 5. Confusion matrix of the 6-vehicle-class classification

Truth \ Estimate	Sedan	Taxi	Van	Minibus	Bus	Truck
Sedan	**78.3%**	3.4%	17.7%	0.6%	0.0%	0.0%
Taxi	0.0%	**100.0%**	0.0%	0.0%	0.0%	0.0%
Van	4.5%	0.0%	**95.5%**	0.0%	0.0%	0.0%
Minibus	0.0%	0.0%	0.0%	**92.3%**	7.7%	0.0%
Bus	0.0%	0.0%	0.0%	0.0%	**100.0%**	0.0%
Truck	0.0%	0.0%	8.0%	8.0%	4.0%	**80.0%**
Overall: 85.6%						

Table 6. Vehicle re-identification accuracy by lane and by vehicle class resulted from (a) Proposed method and (b) Existing method

(a)

	Sedan	Taxi	Van	Minibus	Bus	Truck
Lane 1	50.0%	80.2%	47.9%	62.4%	92.5%	49.7%
Lane 2	48.1%	56.9%	40.1%	75.5%	76.3%	73.3%
Lane 3	37.5%	55.9%	42.2%	76.3%	81.1%	59.8%
Lane 4	29.1%	75.7%	39.2%	60.6%	44.4%	63.8%
All lanes	**42.4%**	**59.8%**	**42.6%**	**70.2%**	**81.2%**	**62.5%**
Overall: 52.4%						

(b)

	Sedan	Taxi	Van	Minibus	Bus	Truck
Lane 1	33.0%	47.2%	33.6%	62.4%	77.9%	47.1%
Lane 2	38.2%	49.2%	35.7%	75.5%	60.1%	58.1%
Lane 3	26.1%	51.4%	17.3%	62.5%	71.5%	42.9%
Lane 4	**2.1%**	**16.9%**	**8.3%**	**27.3%**	**21.3%**	**6.8%**
All lanes	**27.5%**	**46.2%**	**26.5%**	**64.7%**	**66.9%**	**36.8%**
Overall: 37.3%						

Table 7. Hellinger distance between the ground truth and the estimated travel time distributions by lane and by vehicle type resulted from (a) Proposed method and (b) Existing method

(a)

	Small	Other
Lane 1	0.103	0.114
Lane 2	0.124	0.122
Lane 3	0.154	**0.189**
Lane 4	0.155	0.134
All lanes	**0.079**	**0.052**

(b)

	Small	Other
Lane 1	0.077	0.102
Lane 2	0.125	0.184
Lane 3	0.322	0.271
Lane 4	**0.746**	**0.738**
All lanes	**0.290**	**0.296**

Table 8. Mean of estimated travel times (sec) by lane and by vehicle type resulted from (a) Proposed method and (b) Existing method*

(a)

	Small	Other
Lane 1	11.2 (0.3%)	12.0 (0.1%)
Lane 2	13.7 (0.2%)	16.2 (3.7%)
Lane 3	**22.8 (4.1%)**	**19.7 (3.9%)**
Lane 4	53.5 (2.8%)	54.7 (4.0%)
All lanes	**21.7 (2.3%)**	**22.3 (3.9%)**

(b)

	Small	Other
Lane 1	12.4 (11.3%)	12.4 (3.4%)
Lane 2	12.4 (9.7%)	12.4 (26.5%)
Lane 3	12.4 (47.9%)	12.4 (39.6%)
Lane 4	**12.4 (77.5%)**	**12.4 (78.2%)**
All lanes	**12.4 (44.2%)**	**12.4 (46.6%)**

*Values in parenthesis are absolute % errors as compared to ground truth

Table 9. Ground truth mean travel time (sec) of (a) small and (b) other vehicles between lanes

(a)

Travel Time of Small Vehicles between lanes	To Lane 1 (downstream)	To Lane 2 (downstream)	To Lane 3 (downstream)	To Lane 4 (downstream)	Total
From Lane 1 (upstream)	**8.8**	13.4	19.3	/	11.1
From Lane 2 (upstream)	/	**10.9**	26.5	58.8	13.7
From Lane 3 (upstream)	/	13.4	**25.1**	58.3	23.8
From Lane 4 (upstream)	/	17.7	22.4	**57.2**	55.0

(b)

Travel Time of Other Vehicles between lanes	To Lane 1 (downstream)	To Lane 2 (downstream)	To Lane 3 (downstream)	To Lane 4 (downstream)	Total
From Lane 1 (upstream)	**9.1**	15.2	22.8	/	12.0
From Lane 2 (upstream)	/	**12.7**	27.5	56.4	16.9
From Lane 3 (upstream)	/	11.8	**27.0**	51.5	20.5
From Lane 4 (upstream)	/	10.0	29.3	**58.6**	57.1

Table 10. Ground truth number of (a) small and (b) other vehicles between lanes*

(a)

No. of Small Vehicles between lanes	To Lane 1 (downstream)	To Lane 2 (downstream)	To Lane 3 (downstream)	To Lane 4 (downstream)	Total
From Lane 1 (upstream)	157 (61.6%)	78 (30.6%)	20 (7.8%)	0 (0.0%)	255 (100%)
From Lane 2 (upstream)	0 (0.0%)	427 (85.2%)	66 (13.2%)	8 (1.6%)	501 (100%)
From Lane 3 (upstream)	0 (0.0%)	213 (50.5%)	150 (35.5%)	59 (14.0%)	422 (100%)
From Lane 4 (upstream)	0 (0.0%)	3 (1.5%)	9 (4.6%)	184 (93.9%)	196 (100%)

*Values in parenthesis are vehicle proportions for each lane

(b)

No. of Other Vehicles between lanes	To Lane 1 (downstream)	To Lane 2 (downstream)	To Lane 3 (downstream)	To Lane 4 (downstream)	Total
From Lane 1 (upstream)	86 (63.7%)	37 (27.4%)	12 (8.9%)	0 (0.0%)	135 (100%)
From Lane 2 (upstream)	0 (0.0%)	180 (77.3%)	46 (19.7%)	7 (3.0%)	233 (100%)
From Lane 3 (upstream)	0 (0.0%)	91 (59.1%)	47 (30.5%)	16 (10.4%)	154 (100%)
From Lane 4 (upstream)	0 (0.0%)	2 (2.0%)	2 (2.0%)	96 (96.0%)	100 (100%)

*Values in parenthesis are vehicle proportions for each lane

Table 11. Standard deviation of estimated travel times (sec) by lane and by vehicle type resulted from (a) Proposed method and (b) Existing method*

(a)

	Small	Other
Lane 1	7.0 (7.4%)	8.6 (4.0%)
Lane 2	11.2 (6.5%)	13.0 (**10.7%**)
Lane 3	18.2 (10.2%)	15.6 (7.2%)
Lane 4	26.2 (10.2%)	24.2 (1.6%)
All lanes	**21.5 (4.3%)**	**21.2 (1.9%)**

(b)

	Small	Other
Lane 1	6.8 (9.8%)	6.8 (18.4%)
Lane 2	6.8 (35.8%)	6.8 (53.4%)
Lane 3	6.8 (66.6%)	6.8 (53.5%)
Lane 4	6.8 (71.5%)	6.8 (71.6%)
All lanes	**6.8 (67.1%)**	**6.8 (68.7%)**

*Values in parenthesis are absolute % errors as compared to ground truth

List of figures

Figure 1. Video images from different camera views: (a) upstream and (b) downstream

(a) (b)

Figure 2. An illustration of vehicle re-identification on an urban road segment with different lane markings and different vehicle types

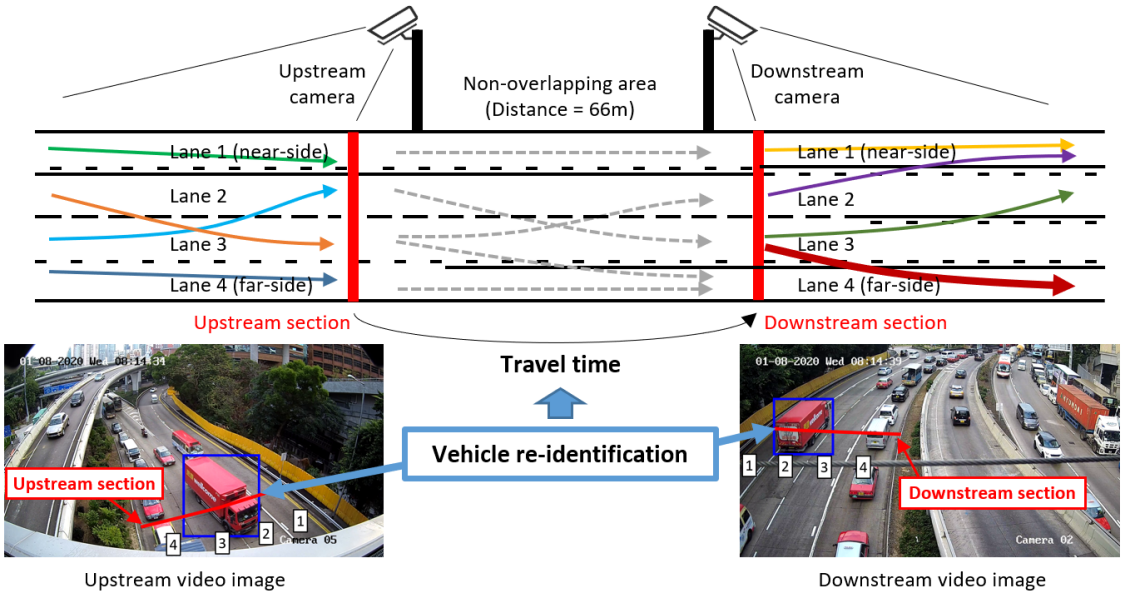

Figure 3. Framework of the proposed methodology

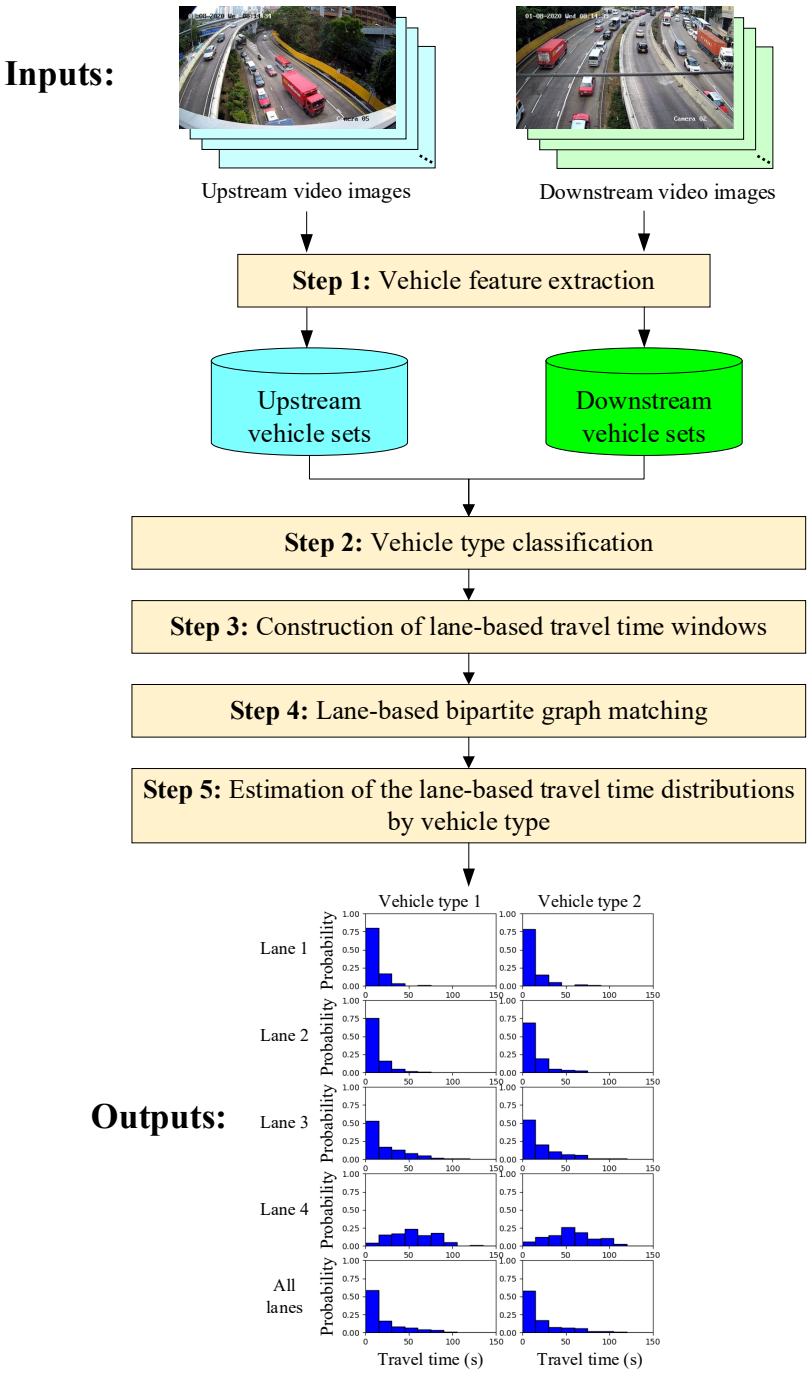

Figure 4. Test site in Hong Kong: (a) Road layout and (b) Site photo

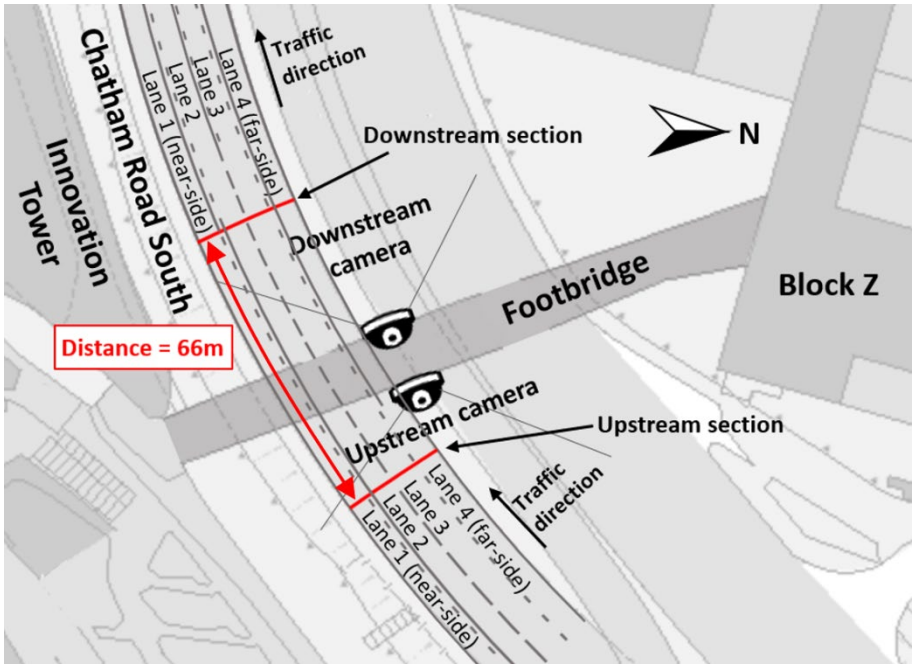

(a)

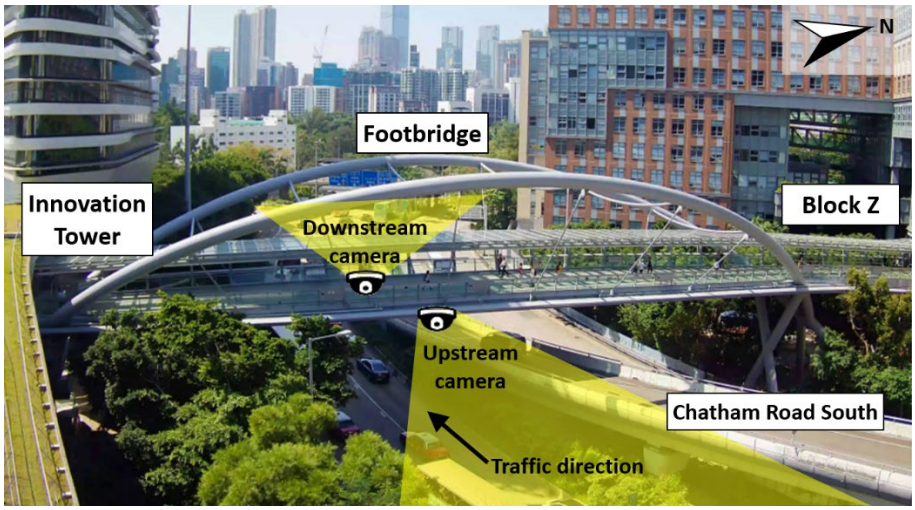

(b)

Figure 5. Travel time distributions by lane and by vehicle type (a) Ground truth (b) Estimated by the proposed method (c) Estimated by the existing method